ELSEVIER

Nuclear Instruments and Methods in Physics Research B 146 (1998) 39–45

NIM B
Beam Interactions with Materials & Atoms

Enhancement of binary encounter electron emission in collisions of highly charged ions with helium gas targets

U. Ramm [a,b,*], U. Bechthold [b,c], O. Jagutzki [b], M. Damrau [a,b], S. Hagmann [b,d], G. Kraft [c], H.D. Böttcher [a], H. Schmidt-Böcking [b]

[a] *Universitätsklinikum, ZRad, Klin. Strahlentherapie, 60596 Frankfurt/Main, Germany*
[b] *Institut für Kernphysik, Universität Frankfurt, 60486 Frankfurt/Main, Germany*
[c] *GSI, 64291 Darmstadt, Germany*
[d] *Department of Physics, Kansas State University, Manhattan Kansas 66502, USA*

Abstract

The energy and angular distribution of δ-electrons produced in collisions of swift heavy ions with helium gas targets are presented. Double differential electron emission cross sections $d^2\sigma/dE_e d\Omega_e$ for different projectiles have been measured as a function of the electron emission energy E_e and the polar electron emission angle ϑ_e. For systematics the cross sections were investigated for different projectiles from neon up to bismuth at ionic charge states between $q = 7+$ and 24+. The specific projectile energy was kept constant within 10%, i.e. $5.4 \leqslant E_P \leqslant 6.0$ MeV/u for the different projectiles. The investigations are focussed on the emission cross sections of the Binary Encounter (BE) electrons. The BE electron emission cross section depends strongly on the ionic q as well as on the nuclear charge state Z_P. At small emission angles ϑ_e the electrons are most enhanced but converging towards the q^2-scaling at larger angles. An appropriate parameter was found to be the ratio of the ionic charge and the nuclear charge q/Z_P. The observation of forward peaked, enhanced electron emission is of great importance for the understanding of radiation damages in dense targets caused by heavy ion collisions.

PACS: 34.50Fa
Keywords: Heavy ion; Ion charge state; Binary encounter electron; Double differential electron emission cross section; Elastic electron scattering

1. Introduction

A prerequisite for the basic understanding of track-structure and in consequence of the biological effects of heavy ion radiation is the knowledge on the mechanism of primary ionization and electron emission processes. The data are required for track-structure calculations and computations of radial dose distributions in collisions of swift heavy ions with matter [1]. Double differential cross sections for the ejection of electrons from helium have been studied intensively for proton

* Corresponding author. Tel.: +49 69 6301 5281; fax: +49 69 6301 5091; e-mail: ramm@ikf007.ikf.physik.uni-frankfurt.de

PII: S0168-583X(98)00481-9

impact (see the references in [2]). Extended experiments on bare heavy ion colliding with gas target verified predictions from simple theories like the First Born and Binary Encounter Approximation (BEA). The electron production scales quadratically with the projectile charge state Z_P^2 [3,4]. In studies on non-bare heavy ion impact unexpected structures in the electron emission energy spectra and deviations of the double differential cross sections from the simple scaling law were found [5,6]. These observations were attributed to changes in screening effects of bound projectile electrons during the collision process.

Typical energy spectra for electron emission resulting from fast heavy ion impact on atomic gas targets are shown in Fig. 1 for the collision system 5.7 MeV/u Ar^{18+}+He. The double differential

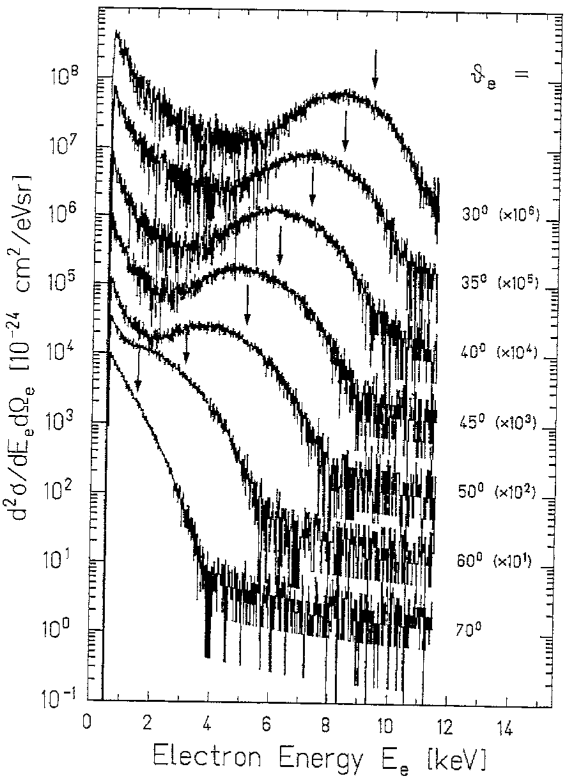

Fig. 1. Double differential cross sections for electrons emission in collisions of 5.7 MeV/u Ar^{18+} with helium. For the emission angles $\vartheta_e = 30°$ up to 70° the spectra are multiplied by the noted numbers. The locations of the BE peak maximum due to the classical two-body collision are indicated by arrows.

electron emission cross sections $d^2\sigma/dE_e d\Omega_e$ are determined for different emission angles $\vartheta_e = 30°$ up to 70°. The spectra are cut off at approximately $E_e = 500$ eV due to the detection efficiency at low energies. The electron emission decreases exponentially for increasing electron energy, exhibiting at higher energies a prominent broad peak, the so-called Binary Encounter peak. Electrons contributing to the exponentially decreasing continuum are well known as resulting from collisions where more than two particles are involved. In these cases, the electrons are simultaneously attracted in the Coulomb potential of both the projectile and the target nucleus. This process has been termed "two-centre electron emission". For more details see Refs. [7–10]. The prominent broad Binary Encounter (BE) peak is due to target electron emission through direct hard collisions with the charged projectile. This electron emission process can be treated as a true two-body encounter process. Regarding the target electron as quasi-free and initially at rest in the laboratory frame, the emission can be denoted in the projectile frame as an elastic electron scattering process in the point-like Coulomb potential of the ion (Rutherford scattering). The classical kinematics result in a maximum energy transfer to a target electron in the laboratory frame

$$E_e = 4\left(\frac{m_e}{m_P}\right)E_P \cos^2\vartheta_e - \Delta E$$

with $0 \leqslant \vartheta_e \leqslant 90°$. (1)

E_e is the final energy of the target electron, E_P the projectile energy, m_e, m_P the electron, and the projectile masses, and ϑ_e the electron emission angle. $\Delta E = 2E_{bind} + \delta E$ is an energy shift due to the binding energy and possible two-centre effects of the projectile and target ions [11]. The width of the BE peak reflects the Compton profile, i.e the momentum distribution of the target electrons due to the orbital motion around the target nucleus. In Fig. 1 the angular dependence of the location of the Binary Encounter peaks calculated from the classsically two-body kinematics are indicated by the arrows. As denoted in Eq. (1) the BE peak shifts to lower electron energies E_e with increasing emission angle ϑ_e.

In the early 1990s Kelbch et al. and Reinhold et al. started a joint experimental and theoretical study of the Binary Encounter electron emission cross sections on the basis of classical electron scattering in the potential of non-bare heavy ions [12,13]. The impulse approximation (IA) was modified using the classical deflection function and a model potential. Screening effects during the electron scattering in the potential of a non-bare uranium ion were taken into account. It was found, that the double peak structure and the enhancement of Binary Encounter electron emission are due to the influence of quantum-mechanical interference phenomenon in the elastic scattering cross section. The Binary Encounter electron production cross sections for non-bare ions were well described by the modified IA model.

In our experiment the energy and angular distributions of δ-electrons produced in collisions of swift heavy ions with helium gas targets are studied. Double differential electron emission cross sections $d^2\sigma/dE_e d\Omega_e$ for different projectiles have been measured as a function of the electron emission energy E_e and the polar electron emission angle ϑ_e. For systematics the cross sections were investigated for different projectiles from neon up to bismuth at ionic charge states between $q = 7+$ and 24+. The specific projectile energy was kept constant within 10%, i.e. $5.4 \leqslant E_P \leqslant 6.0$ MeV/u for the different projectiles. Thus, at this certain projectile energy the ratio of the ionic charge q to the nuclear charge Z_P seems appropriate to describe the influence of screening of elastic electron scattering in swift heavy ion atom collisions. The ratio varied widely between $q/Z_P = 0.3$ and 1. The investigations are focussed on the emission cross sections of the Binary Encounter electrons.

2. Experiment

The experiment for evaluating the double differential electron emission cross sections was performed at the UNILAC-accelerator at the GSI (Darmstadt, FRG). The heavy ion beam is collimated to a spot size of 0.2×0.2 mm within 3 m before entering the scattering chamber. The beam passes through the aperture (2 mm diameter) of a differentially pumped static gas target. The gas-cell consists of two concentrical tubes mounted perpendicular to the beam axis. The ejected electrons emerge from the gas cell through a slit of 1 mm height. This compact construction of the gas-cell allows to operate at a pressure ratio of 1000:1 between the gas-cell and the scattering chamber. Single collision conditions are maintained keeping the target gas at low pressure, typically 5 m Torr corresponding to 5×10^{-6} Torr in the scattering chamber. The beam current of max. 800 pA is monitored in a shielded Faraday-Cup and digitized for normalization of the electron counting rate to a constant number of particles. Electrons ejected from the target region are measured at various angles using a 90° electrostatic hemispherical sector analyzer. The analyzer is mounted rotatable to the center of the gas-cell. This yields an observation angle between $\vartheta_e = 30°$ and 90° with respect to the beam axis. The voltage scan of the analyzer is driven by the digitized beam current. This procedure eliminate any influence of beam fluctuation on the shape of the spectra. Since the observed target length varies with the observation angle and is proportional to $(\sin\vartheta_e)^{-1}$, the spectra are multiplied with the corresponding correction factor. The electrons are detected by a single channel electron multiplier (channeltron), mounted at the focal point of the analyzer. The channeltron signals are electronically processed and recorded by a multichannel analyzer. A personal computer system stores the electron data for further treatment.

The pressure in the gas-cell, the transmission rate of the analyzers and the efficiency of the channeltrons are not known precisely. Thus, the relative cross sections of the collision system 3.6 MeV/u Ni^{22+} on He are normalized to the absolute data taken from a very similar collision system of Schneider et al. (3.5 MeV/u Fe^{22+} on He) [9]. Due to the accuracy of the iron data, the normalization procedure yields an absolute uncertainty of the cross sections of about 40%. The deduced relative uncertainties in the cross sections are estimated to be around 10% resulting from statistical error and slight experimental drifts e.g. in the zero-point of the target pressure control setup.

3. Theory of elastic electron scattering cross section

Experimental and theoretical investigations on Binary Encounter electron emission from collisions of non-bare heavy ions with gas targets have been started in the early 1990s by Kelbch et al. and Reinhold et al. [12,13]. A modified IA has been applied to describe the structures in electron emission spectra and the deviations of double differential electron emission cross sections from the simple scaling law. Within the IA, the BE electron emission process is treated in the projectile frame, where it is considered as an elastic scattering of quasi-free target electrons in the screened potential of the non-bare projectile in rest. From the simple relation $\Theta_e = 180^\circ - 2\vartheta_e$ electron emission into forward angle $\vartheta = 0^\circ$ relates to backward scattering $\Theta_e = 180^\circ$ in the CM-system. For comparison the experimental double differential cross sections $d^2\sigma/dE_e d\Omega_e$ and the observation angles ϑ_e have to be transformed into the projectile frame. In the case of electron scattering the projectile frame is in a first approximation the same as the centre-of-mass system (CM), resulting in the simple relation:

$$\left[\frac{d^2\sigma}{dE_e^{CM} d\Omega_e}\right]_{BE}^{CM} = \left[\frac{d^2\sigma}{dE_e d\Omega_e}\right]_{BE}^{LS} \sqrt{E_e^{CM}/E_e}, \quad (2)$$

$$E_e^{CM} = (m_e/m_P)E_P, \quad (3)$$

where the electron energy in the projectile frame E_e^{CM} is given by the projectile energy E_P and the mass ratio of the electron and the projectile only. The electron emission scattering cross sections in the CM-system are calculated from the classical deflection function considering a screened potential. A non-Coulomb-like model potential suggested by Green and Garvey in 1975 [14] was used for calculations. The potential, in the following referred to as Green–Garvey potential, has the following analytical form [14]:

$$V(r) = 2[(N-1)(1-\Omega_S(r)) - Z_P]\frac{1}{r} \quad (4)$$

$$\text{with} \quad \Omega_S(r) = \left[\frac{\eta}{\xi}(e^{\eta r} - 1) + 1\right]^{-1},$$

where Z_P is the nuclear charge of the ion and N is the number of remaining electrons. The two screening parameters η and ξ are calculated and tabulated in Ref. [14]. The Green–Garvey potential $V(r)$ gives rise to a deflection function extending scattering angles in the centre-of-mass system larger than $\Theta_e \geq 180^\circ$. Thus, the structure in the electron spectra and the enhancement of Binary Encounter electron emission is due to the influence of quantum-mechanical interference phenomenon in the elastic scattering cross sections.

Quantum-mechanical calculations of BE electron emission using the Green–Garvey potential has been applied to numerous ions ($Z_P = 6, 9, 26, 53, 92$) at various charge states for impact energies between 0.1 and 100 MeV/u by Schultz et al. [11]. They worked out, that the structures in the BE peak and the enhancement of the electron emission is a characteristic of each nuclear species and results in a strong dependence on the ionic charge and energy as well as on the scattering angle. At a certain projectile energy E_P, within the given region, the observations were most pronounced for small q/Z_P ratios and forward observation angles ϑ_e. The calculations reproduced well data of experiments on electron emission performed by Wolff et al. [15,16] and Hagmann et al. [17]. Good agreement was obtained for selected heavy ion atom collisions at energies below $E_P \leq 1.0$ MeV/u.

4. Results and discussion

In Fig. 2 energy spectra for electron emission resulting from heavy ion impact on a helium gas target are summarized for different projectiles, neon up to bismuth, at one given emission angle $\vartheta_e = 35^\circ$. All spectra exhibit the expected exponentially decreasing shape due to "two-centre electron emission", superimposed by the broad peak of Binary Encounter electrons. The expected locations of the BE peak calculated from the classical relationship given in Eq. (1) are indicated by the arrows. The variation of the BE peak position is due to the slight variation of the projectile energy E_P and the energy shift ΔE. The shapes of the Binary Encounter peak differ due to possible two-centre effects of projectile and target ions [11].

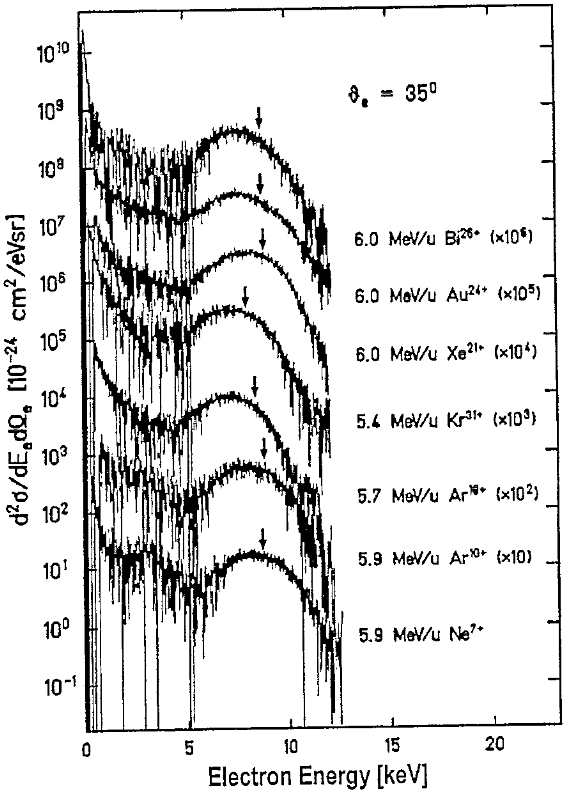

Fig. 2. Double differential cross section of electron emission from collisions of fast heavy Ne-, Ar-, Kr-, Xe-, Au-, and Bi-ions with helium at one given emission angle $\vartheta_e = 35°$. The projectile energy varies slightly within the different collision systems $5.4 \leqslant E_P \leqslant 6$ MeV/u. The spectra are multiplied by the noted numbers.

For light and partially stripped ions (Ne^{7+} and Ar^{10+}) the so-called loss peak from projectile electrons stripped of in the collision are seen in the intermediate energy range [7]. The mean energy of these loss electrons corresponds to the velocity of the projectiles $v_e = v_P$ (v_e and v_P are the projectile and electron velocities, respectively). For bare and highly stripped ions (Ar^{18+} and Kr^{31+}) no such peak is seen. The peak shape and the dependence on the emission angle is due to the Compton profile of the projectile electrons. Thus, for heavy ions, where the Compton profile is small, the loss peak is visible at forward emission angles ($\vartheta_e \leqslant 30°$) only.

In order to compare the single differential cross section of the BE electron emission with those from the elastic scattering of quasi-free electrons in the centre-of-mass system the experimental double differential cross sections were transformed using Eq. (2). For each scattering angle θ_e in the projectile frame (i.e. observation angle ϑ_e in the laboratory frame) the BE peak is separated from other components by a fit procedure to the two-centre electrons. The decreasing continuum is described by an exponential function and subtracted from the energy spectra, leaving the BE peak only. The data are integrated over the Binary Encounter peak, yielding the single differential cross section $d\sigma/d\Omega^{CM}_{eBE}$. Fig. 3 shows the single differential cross section $d\sigma/d\Omega^{CM}_{eBE}$ versus the projectile charge state q for six different emission angles between $\vartheta_e = 30°$ and 60°. Since the projectile energy varies by a factor of approx. 10% within the different experiments the cross sections are multiplied with E_P^2 due to the predicted scaling of the elastic electron scattering. The broken and dotted-broken lines indicate the elastic scattering cross section of a quasi-free electron in the Coulomb-like projectile potential at two selected observation angles. The Rutherford scattering cross sections are multipled by 2 to account for the two electrons of the helium target. In the centre-of-mass system the two lines correspond to scattering angles $\Theta_e = 120°$ ($\vartheta_e = 30°$) and $\Theta_e = 60°$ ($\vartheta_e = 60°$). From Eq. (3) an electron energy in the projectile frame of

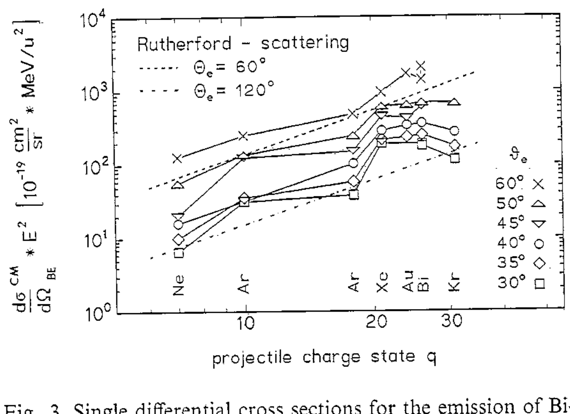

Fig. 3. Single differential cross sections for the emission of Binary Encounter electron emission from helium induced by various projectiles. Broken lines: Rutherford-scattering cross section of free electrons with $E_e^{CM} = 544$ eV in the potential of a pointlike charge q at $\Theta_e = 120°$, $\vartheta_e = 30°$ (down) and $\Theta_e = 60°$, $\vartheta_e = 60°$ (above).

$E_e^{CM} = 3270$ eV is calculated for all ion helium collision systems with projectile energies around $E_P \approx 6$ MeV/u.

In general, the BE cross sections derived from the energy spectra increase with increasing projectile charge state. For light and highly stripped ions (Ne^{7+}, Ar^{18+}, and Kr^{31+}) the single differential cross section agree quite well to the elastic scattering cross section. For the heavier, non-bare ions a strong deviation of the Binary Encounter electron emission data is seen. The enhancement is most pronounced at small emision angles and decreases with increasing observation angle ϑ_e (the deviation at high observation angles $\vartheta_e \approx 60°$ is due to the uncertainty in the separation of the cross sections due to the soft collision and BE electron emission process (see Fig. 1)). For a more accurate illustration of the dependence on screening effects on electron scattering in non-bare projectile potentials Fig. 4 shows the cross section of the Binary Encounter electron emission for various emission angles versus the parameter q/Z_P. At a given projectile energy E_P the ratio of the ionic q to the nuclear charge Z_P is appropriate to indicate the strength of the diffraction pattern due to the screening of the nuclear charge ($q/Z_P = 1$ stands for the identity of the ionic and the nuclear charge, i.e. fully stripped ions and elastic electron scattering conditions). The cross sections are normalized to those taken from the data of the fully stripped Ar^{18+}–ion ($q = 18+$, $E_P = 5.7$ MeV/u). The horizontal line indicates the elastic Rutherford electron scattering cross sections. The open symbols in Fig. 4 are taken from theoretical study of Schultz et al. [11]. The single differential cross sections $d\sigma/d\Omega_{eBE}^{CM}$ are calculated using the modified IA for electron scattering in Fe^{11+}- and J^{21+}-potentials. The electron energy corresponds to the projectile energy $E_P = 5$ MeV/u. The iodine data are very similar to the collision system Xe^{21+} on helium. The ratios q/Z_P is identically, the energies differ by a factor of 12% only. Good agreement is obtained for the measured BE electron emission and calculated electron scattering data.

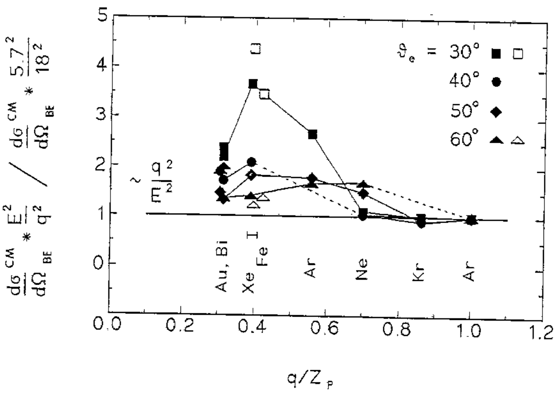

Fig. 4. Relative projectile charge state (q/Z_P) dependence of normalized single differential cross section of Binary Encounter electrons in the centre-of-mass system. Solid symbols: this work; open symbols: taken from Schultz et al. [11]; horizontal solid line: Rutherford-scattering of a quasi-free electron in the Coulomb potential of a point-like ion.

The normalization on the Ar^{18+} data points out the dependence of BE electron emission cross sections on screening effects. The data approach the identity with the elastic electron scattering for highly charged ions ($q/Z_P \geqslant 0.7$). The most pronounced deviation from the elastic electron scattering appears at forward peaked emission $\vartheta_e = 30°$ when the ratio tends to a minimum. For decreasing ratio q/Z_P, where screening effects are increasing, the enhancement exhibits a maximum around $q/Z_P \approx 0.4$. For larger observation angles enhancement becomes smaller, electron scattering is caused by a point-like projectile charge q only.

5. Conclusions

In this presentation the Binary Encounter electron emission cross sections are reported for highly charged and partially stripped ions at extended impact energy E_P and heavy ions up to bismuth. The BE electron emission cross section depends strongly on the ionic q as well as on the nuclear charge state Z_P. At small emission angles ϑ_e the electrons are most enhanced but converging towards the q^2-scaling at larger angles. An appropriate parameter was found to be the ratio of the ionic and the nuclear charge q/Z_P. The observation of forward peaked, enhanced electron emission is of large importance for the understanding of radiation damages in dense targets caused by heavy ion collisions.

Acknowledgements

This work was supported by the Gesellschaft für Schwerionenforschung (GSI, FRG), the Bundesministerium für Forschung und Technologie (BMFT, FRG) and the Chemical Sciences Division of Basic Energy Sciences, US Department of Energy (DOE, USA).

References

[1] G. Kraft, M. Krämer, Adv. in Radiat. Biol. 17 (1993) 1.
[2] M.E. Rudd, L.H. Toburen, N. Stolterfoht, Atom. Data and Nucl. Data Tables 18 (1976) 413.
[3] D.H. Lee, P. Richard, T.J.M. Zouros, J.M. Sanders, J.L. Shinpaugh, H. Hidmi, Phys. Rev. A 41 (1990) 4816.
[4] U. Ramm, U. Bechthold, O. Jagutzki, S. Hagmann, G. Kraft, H. Schmidt-Böcking, Nucl. Instr. and Meth. B 98 (1995) 359.
[5] C. Kelbch, R.E. Olson, S. Schmidt, H. Schmidt-Böcking, S. Hagmann, J. Phys. B: At. Mol. Opt. Phys. 22 (1989) 2171.
[6] P. Richard, D.H. Lee, T.J.M. Zouros, J.M. Sanders, J.L. Shinpaugh, J. Phys. B: At. Mol. Opt. Phys. 23 (1990) L213.
[7] N. Stolterfoht, D. Schneider, D. Burch, H. Wiemann, J.S. Risley, Phys. Rev. Lett. 33 (1974) 59.
[8] J.O.P. Pedersen, P. Hvelplund, A.G. Petersen, F. Fainstein, J. Phys. B: At. Mol. Opt. Phys. 23 (1990) L597.
[9] D. Schneider, D.R. DeWitt, R.W. Bauer, W.G. Graham, A.S. Schlachter, B. Skogvall, P. Fainstein, R.D. Rivarola, Phys. Rev. A 46 (1992) 1296.
[10] J.H. Macek, Nucl. Instr. and Meth. B 53 (1991) 416.
[11] D.R. Schultz, R.E. Olson, J. Phys. B: At. Mol. Opt. Phys. 24 (1991) 3409.
[12] C. Kelbch, R. Koch, S. Hagmann, K. Ullmann, H. Schmidt-Böcking, C.O. Reinhold, D.R. Schultz, R.E. Olson, G. Kraft, Z. Phys. D 22 (1992) 713.
[13] C.O. Reinhold, D.R. Schultz, R.E. Olson, C. Kelbch, R. Koch, H. Schmidt-Böcking, Phys. Rev. Lett. 66 (1991) 1842.
[14] R.H. Garvey, C.H. Jackmann, A.E.S. Green, Phys. Rev. A 12 (1975) 1144.
[15] W. Wolff, J.L. Shinpaugh, H.E. Wolf, R.E. Olson, J. Wang, S. Lencinas, D. Piscevic, R. Herrmann, H. Schmidt-Böcking, J. Phys. B: At. Mol. Opt. Phys. 25 (1992) 3683.
[16] W. Wolff, J.L. Shinpaugh, H.E. Wolf, R.E. Olson, U. Bechthold, H. Schmidt-Böcking, J. Phys. B: At. Mol. Opt. Phys. 26 (1993) L64.
[17] S. Hagmann, W. Wolff, J.L. Shinpaugh, H.E. Wolf, R.E. Olson, C.P. Bhalla, R. Shingal, C. Kelbch, R. Herrmann, O. Jagutzki, R. Dörner, R. Koch, J. Euler, U. Ramm, S. Lencinas, V. Dangendorf, M. Unverzagt, R. Mann, P. Mokler, J. Ullrich, H. Schmidt-Böcking, C.L. Cocke, J. Phys. B: At. Mol. Opt. Phys. 25 (1992) L287.